Planta (2000) 212: 75–84

Planta

Cellular compartmentation of cadmium and zinc in relation to other elements in the hyperaccumulator *Arabidopsis halleri*

Hendrik Küpper[1], Enzo Lombi[2], Fang-Jie Zhao[2], Steve P. McGrath[2]

[1] Universität Konstanz, Mathematisch-Naturwissenschaftliche Sektion, Fachbereich Biologie, Fach M665, 78457 Konstanz, Germany
[2] IACR-Rothamsted, Soil Science Department, Harpenden, Herts., AL5 2JQ, UK

Received: 4 April 2000 / Accepted: 16 May 2000

Abstract. The cellular compartmentation of elements was analysed in the Zn hyperaccumulator *Arabidopsis halleri* (L.) O'Kane & Al-Shehbaz (= *Cardaminopsis halleri*) using energy-dispersive X-ray microanalysis of frozen-hydrated tissues. Quantitative data were obtained using oxygen as an internal standard in the analyses of vacuoles, whereas a peak/background ratio method was used for quantification of elements in pollen and dehydrated trichomes. *Arabidopsis halleri* was found to hyperaccumulate not only Zn but also Cd in the shoot biomass. While large concentrations of Zn and Cd were found in the leaves and roots, flowers contained very little. In roots grown hydroponically, Zn and Cd accumulated in the cell wall of the rhizodermis (root epidermis), mainly due to precipitation of Zn/Cd phosphates. In leaves, the trichomes had by far the largest concentrations of Zn and Cd. Inside the trichomes there was a striking sub-cellular compartmentation, with almost all the Zn and Cd being accumulated in a narrow ring in the trichome base. This distribution pattern was very different from that for Ca and P. The epidermal cells other than trichomes were very small and contained lower concentrations of Zn and Cd than mesophyll cells. In particular, the concentrations of Cd and Zn in the mesophyll cells increased markedly in response to increasing Zn and Cd concentrations in the nutrient solution. This indicates that the mesophyll cells in the leaves of *A. halleri* are the major storage site for Zn and Cd, and play an important role in their hyperaccumulation.

Key words: *Arabidopsis* (Cd, Zn accumulation) – Cadmium accumulation – Cellular compartmentation – Hyperaccumulation (heavy metals) – Trichome – Zinc accumulation

Abbreviations: EDXA = energy dispersive X-ray analysis; SEM = scanning electron microscope

Correspondence to: S. P. McGrath;
E-mail: steve.mcgrath@bbsrc.ac.uk; Fax: +44-1582-760981

Introduction

Many heavy metals, e.g. Cu, Zn, Ni, Co and Mn, are essential trace elements for plants, but can be highly toxic when present at large concentrations. For most plant species, the range of beneficial concentrations of these metals is often very narrow (Marschner 1995). Other heavy metals such as Cd are not essential and are also highly toxic.

Plants have developed different tolerance strategies to grow on soils rich in heavy metals. A large number of tolerant plants are so-called "excluders": they are able to restrict root uptake, and in particular, root-to-shoot translocation of heavy metals (Baker 1981). Some plant species, however, have developed a strategy that is the opposite to that of the "excluders": they accumulate heavy metals to exceedingly high levels in the aboveground parts. The term "hyperaccumulator" was introduced by Brooks et al. (1977) for plants that accumulate more than 1 mg Ni per gram of dry weight in their shoots in their natural habitats. To date, more than 400 species of hyperaccumulators belonging to 45 families have been identified, of which about 75% are Ni-hyperaccumulators (Brooks 1998; Baker et al. 2000). So far, about 18 species of Zn-hyperaccumulator have been identified. A Zn-hyperaccumulator is defined as a plant that accumulates at least 10 mg Zn per gram of dry weight in shoots in its natural habitat (Brooks 1998). *Thlaspi caerulescens* J.&C. Presl (Brassicaceae) is the best-known Zn-hyperaccumulator (Baker et al. 2000). This species can also hyperaccumulate Cd (>0.1 mg g^{-1} dry weight of shoots), although recent results showed that different ecotypes of *T. caerulescens* varied greatly in their capacity to take up Cd (Lombi et al. 2000). Driven by the potential of their use to extract and remove toxic metals from contaminated soils (McGrath 1998; Salt et al. 1998), there has been recent progress in our understanding of the uptake, translocation and compartmentation of heavy metals, particularly in Ni-hyperaccumulators in the genus *Alyssum* and in *T. goesingense* (Krämer et al. 1997; Salt et al.

2000), and in the Zn-hyperaccumulator *T. caerulescens* (Lasat et al. 1996, 2000; Shen et al. 1997; Küpper et al. 1999; Salt et al. 1999).

Although *Arabidopsis halleri* (L.) O'Kane & Al-Shehbaz (previously known as *Cardaminopsis halleri*) has long been known as a Zn-hyperaccumulator (Brooks 1998), there have been very few studies on the uptake, tolerance and cellular compartmentation of the metal in this species. By crossing *A. halleri* with a non-hyperaccumulating, non-tolerant species *Arabidopsis petraea*, Macnair et al. (1999) found that Zn tolerance and hyperaccumulation are genetically independent characters. A recent study showed that *A. halleri* can accumulate up to 32 mg g^{-1} Zn in shoots without suffering from phytotoxicity in hydroponic culture, and that Zn is accumulated preferentially in the trichomes (Zhao et al. 2000). These preliminary results suggested that the cellular compartmentation of Zn in *A. halleri* is very different from that found in *T. caerulescens* leaves (Küpper et al. 1999).

The aim of the present study was to quantify the cellular distribution of both Zn and Cd in different tissues of *A. halleri*. A new method was developed to allow in-situ quantitative measurements of Cd and Zn in vacuoles. Furthermore, we investigated the responses in terms of cellular distribution of Zn, Cd and other major elements to different Zn/Cd treatments in nutrient solution.

Materials and methods

Plant culture

Seeds of *Arabidopsis halleri* (L.) O'Kane & Al-Shehbaz were germinated on a mixture of perlite and vermiculite moistened with deionised water. Three weeks after germination, seedlings were transferred to 1-L vessels containing (in μM) 1000 $Ca(NO_3)_2$, 500 $MgSO_4$, 50 K_2HPO_4, 100 KCl, 10 H_3BO_3, 1.8 $MnSO_4$, 0.2 Na_2MoO_4, 0.31 $CuSO_4$, 0.5 $NiSO_4$, 50 Fe(III)-HBED (Fe(III)-N,N′-bis(2-hydroxybenzyl)-ethylenediamine-N,N′-diacetate), and 5 $ZnSO_4$ (Shen et al. 1997). Solution pH was maintained at around 6.0 with 2000 μM Mes (2-morpholinoethanesulphonic acid, 50% as potassium salt). Three weeks later the chelating agent for Fe was changed to EDDHA [ethylenediamine-di(*o*-hydroxyphenylacetic acid)]. There were four Zn/Cd treatments: Control (5 μM Zn, no addition of Cd); 500 μM Zn, no addition of Cd; 5 μM Zn, 100 μM Cd; and 500 μM Zn, 100 μM Cd. Both Zn and Cd were added as sulfates, i.e. as divalent cations. As both ions are biologically redox-inert, this will also be their oxidation state inside the plants. However, since energy-dispersive X-ray microanalysis (EDXA) does not provide information about oxidation states of the elements measured, throughout the following they will be mentioned as Zn/Cd instead of Zn^{2+}/Cd^{2+}.

Each treatment was replicated in three vessels, each containing four plants. The treatments were started 2 weeks after seedlings were transferred to hydroponics. The nutrient solution was aerated continuously and renewed every 3 d until the plants were flowering (14 weeks). Plants were grown in a controlled environment room with the following conditions: 16 h day length with a photon flux density of 350 μmol m^{-1} s^{-1} supplied by fluorescent tubes, 20 °C/16 °C day/night temperature, and 60–70% humidity.

Freeze-fracturing and EDXA

Sections of plant tissue were excised and mounted in a stainless-steel vice, or, when leaf surfaces with trichomes were analysed, mounted flat on the surface of carbon stubs using conductive carbon tabs. Samples were then rapidly (within less than a minute after excision) frozen in melting nitrogen slush and transferred to a fracturing chamber cooled to −170 °C. For root and leaf cross-sections, a blade was used to cut through the cells rather than breaking the tissue at the cell surfaces. Subsequently, samples were evaporatively coated with carbon to produce an electrically conductive surface and thus prevent charging under the electron beam. Carbon was used instead of metal coating to avoid interference on the elements measured. Energy dispersive X-ray analysis was performed in a scanning electron microscope (SEM; Philips XL 40) on a cryostage (−160 °C to −180 °C), using an acceleration voltage of 30 kV and a working distance of 10 mm. With this accelerating voltage, the maximum penetration depth of the electron beam is about 10 to 15 μm (leading to a vertical resolution of 5–8 μm). In contrast, the horizontal resolution (determined mainly by the diameter of the electron beam) is better than 1 μm. Hence, differences in concentration, e.g. between small organelles such as chloroplasts or mitochondria and the cytoplasm cannot be resolved. However, differences between the cell wall and the vacuole can be assessed if the cell wall being measured is approximately parallel to the electron beam.

The distribution of Zn across a section of a sample was measured semi-quantitatively by displaying the count rate within a narrow spectrum window within its peak (0.6 × peak half-width) along a transect line. A two-dimensional distribution pattern was also recorded by scanning an area of the specimen repeatedly for up to 2 h and integrating the counts for Zn, Cd, Ca and K within their respective spectrum windows into dot-maps. In both line and area scans, the spectrum-analysis software did not allow for the separation of the element-specific X-rays (net peak counts) from the background counts. Therefore, these scans were performed only on those elements with a peak/background ratio greater than two. A dot-map of oxygen distribution was recorded before analysis of the specimen. Because of its low energy, the X-rays emitted by oxygen are most strongly affected by shading (caused by the vice or neighboring cells) inside the sample, so that an oxygen dot-map clearly shows these shaded parts of the sample. The regions of specimen that suffered from shading effects were not used for quantitative analysis. Additionally, the collection of oxygen dot-maps enabled the distinction between hydrated (living) and dry (dead) trichomes.

Spectra from 0 to 20 keV were collected at increments of 10 eV per channel with the electron beam focused on a rectangular area in the centre of selected cells. The spectra were analysed using the program Superquant (EDAX, San Francisco, Calif., USA), which separates the background from the element-specific peaks and fully deconvolutes the spectra for the correction of interference between elements. Thus, the analysis with this program yielded the net peak count rate and the peak/background ratio for each element, which were used for quantification as described below.

For quantification of EDXA data in a biological sample of unknown composition, usually a known amount of substance which is not present in the sample (e.g. a rare element like Rb) is added as an internal standard (e.g. Tomos et al. 1994). The use of an internal standard is necessary because the net count rate (counts/s) inside the X-ray emission peak depends not only on the concentration of the element, but also on the working distance, the beam current, and the shape of the specimen. Additionally, at higher concentrations the count rates are saturating (Fig. 1A and B). Although adding an internal standard to overcome these problems represents a possible solution for samples extracted from a tissue by the use of micropipettes (Tomos et al. 1994; Küpper et al. 1999), it is not suitable for in situ analysis of biological samples. Additionally, only very few types of tissue are accessible to sampling with micropipettes.

In this study, we used the signal of endogenous oxygen as an internal standard to quantify the concentrations of several elements in frozen hydrated samples. This approach is based on the fact that the vacuole of a living cell contains about 80–90% water. Hence, we assumed that every vacuole contained 85% water, allowing up

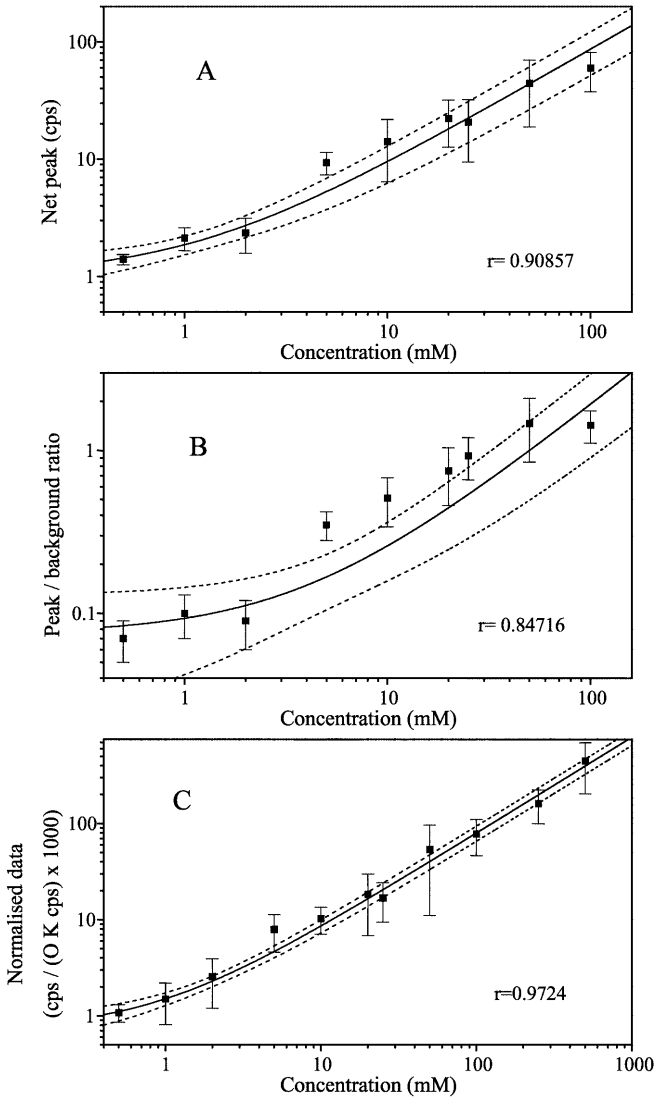

Fig. 1A–C. Comparison of methods for using EDXA data as a quantitative measure of in-situ element concentrations in frozen multi-element standards. For all elements except Cd, the Kα X-ray emission lines were used for quantification. In this figure for Cd, the Lα line was used instead because of the high energy of the Kα line of this element. The graphs were obtained by linear regressions with error bars as weights. **A** Net peak counts. **B** Peak/background ratio. **C** Net peak counts/oxygen net peak counts

to ±10% error. This method extended the linear portion of the calibration curve to much higher concentrations (Fig. 1C), because the effects of instrumental conditions on element-specific peak counts were cancelled out by similar effects on oxygen. The quantification was calibrated (to obtain the element-specific emission efficiency) using multi-element standards. Hence the final formula for quantification of an element was obtained as: (net peak counts) × (emission efficiency) × (net oxygen counts)$^{-1}$. Using this method, a reliable quantification (±15%) within the concentration range 5–500 mM was achieved for Zn, Ca, Cd, Cl, K, Mg and P. The data for Cd are shown as an example in Fig. 1C.

For samples that have a highly variable or low water content (e.g. pollen, dehydrated trichomes), the reliability of the method is less certain. In these cases, a calibration between peak/background ratios for specific elements and their concentrations in the standard solutions was used to quantify the data recorded (Boekestein et al. 1984; Van Steveninck and Van Steveninck 1991). In such samples, the term "concentration" refers to the apparent concentration of the element, meaning that not all of this is in soluble form.

Determination of element concentrations in whole plant tissues

Plants were harvested after growing on different treatments for 14 weeks. The plants were divided into roots and shoots, washed with deionised water and blotted dry. The samples were then oven-dried for 72 h and dry weights determined. Dried samples were ground and a 0.2-g sub-sample was digested with a mixture of HNO_3 and $HClO_4$. Concentrations of Cd, Zn and other elements in the digests were determined using inductively coupled atomic emission spectrometry (ICP-AES; Fisons ARL Accuris).

Results

Plant growth and elemental composition

Visual observations of the plant growth showed healthy growth of plants in all treatments except 5 μM Zn + 100 μM Cd. Plants in this treatment were chlorotic. The observations of growth were confirmed by the biomass data at the end of the experiment: while the treatments with 500 μM Zn and 500 μM Zn + 100 μM Cd showed no significant (*t*-test, $P > 0.05$, $n = 9$) differences compared to the control (5 μM Zn), the plants treated with 5 μM Zn + 100 μM Cd had approximately 40% reduced shoot and 60% reduced root biomass (Table 1).

With 5 μM Zn in the nutrient solution, Zn was primarily accumulated in the shoots. At the higher Zn concentration (500 μM Zn), the concentration of Zn in the roots exceeded that in the shoots. This was probably due to precipitation in the root apoplast. In comparison, the Cd concentration in roots was always larger than in shoots. When either Cd or Zn was present in the nutrient solution at large concentrations (100 μM Cd + 5 μM Zn, 500 μM Zn), the plants accumulated almost 6,000 mg Cd kg^{-1} or 9500 mg Zn kg^{-1} in the shoots (Table 1). In the treatments with 100 μM Cd, increasing Zn from 5 to 500 μM decreased the Cd concentration in the shoots by half. This probably explains why phytotoxicity only occurred in the 5 μM Zn + 100 μM Cd treatment.

Concentrations of other elements were influenced by the different treatments (Table 1). All treatments with elevated Zn or Cd concentrations led to a decrease of Mn and Fe in the shoots. In contrast, the shoot concentration of S increased in both Cd treatments, especially in the plants grown in 5 μM Zn + 100 μM Cd. In this treatment, the shoot concentration of Mg was also significantly (*t*-test, $P < 0.001$, $n = 6$) increased compared to the control. In the roots, all treatments with elevated Cd or Zn showed an increase in P concentrations, with a maximum in the 500 μM Zn + 100 μM Cd treatment.

X-ray microanalysis of frozen-hydrated tissues

Roots. In the control treatment the average concentrations of Zn and Cd in roots were below the detection limit of EDXA (i.e. < 5 mM). However, in the 100 μM

Table 1. *Effects of Zn and Cd treatments on shoot and root dry weights, and the concentrations of various elements in A. halleri.* Standard deviations are in parentheses

Plant part	Treatment	DW (g pot^{-1})	Concentration (mg kg^{-1})						
			Cd	Zn	Fe	Mg	Mn	P	S
Shoot	5 µM Zn	14.2 (4.0)	8 (1.4)	685 (138)	203 (34)	4414 (560)	165 (13)	3691 (571)	9517 (2073)
	500 µM Zn	16.5 (0.5)	73 (18)	9491 (738)	155 (44)	4006 (424)	77 (6)	3204 (115)	9451 (1372)
	500 µM Zn + 100 µM Cd	12.9 (2.1)	2740 (460)	7429 (1061)	166 (27)	4981 (200)	98 (24)	3223 (277)	11700 (1354)
	5 µM Zn + 100 µM Cd	6.2 (2.6)	5722 (1334)	1202 (356)	149 (21)	6326 (681)	108 (10)	4329 (272)	14031 (891)
Root	5 µM Zn	4.2 (0.6)	22.9 (19.2)	392.9 (130)	3092 (793)	2908 (107)	340 (121)	7658 (533)	7765 (508)
	500 µM Zn	5.1 (1.7)	27.8 (4.5)	57145 (9786)	4027 (758)	3220 (74)	552 (123)	24739 (2935)	7727 (848)
	500 µM Zn + 100 µM Cd	4.3 (0.9)	24116 (4512)	68341 (9061)	4407 (513)	3223 (921)	444 (86)	30975 (3025)	7935 (1773)
	5 µM Zn + 100 µM Cd	0.9 (0.4)	37350 (4575)	1061 (86)	16834 (4149)	6769 (3132)	734 (257)	18841 (357)	10357 (2088)

Cd treatment a gradient was found with the highest Cd concentrations in the rhizodermal (root epidermal) cell walls and the lowest in the central cylinder (Table 2). In the 500 µM Zn treatments (with or without 100 µM Cd), the outer cell wall of the root rhizodermis accumulated so much Zn that the peak/background ratio was high enough for recording dot-maps and line-scans of Zn distribution (Fig. 2). The dot-maps clearly showed bright spots of Zn accumulation, which correlated with high concentrations of P. Additionally, the line-scans (Fig. 2) and quantitative analyses (Table 2) showed that there was a second, smaller peak of P concentration in the central cylinder, which did not relate to the Zn concentration. Concentrations of Zn and Cd in all parts of the roots, except the outer epidermal cell walls, were at or below the detection limit of EDXA (i.e. <5 mM).

Leaves. As displayed quantitatively in Fig. 3, the highest Zn and Cd concentrations were found in the bases of trichomes on the leaf surface. A closer view shows that this accumulation was restricted to a very narrow area in the upper part of the trichome base (Fig. 4). Concentrations of Zn and Cd in this compartment can be higher than 1 M (Fig. 3). Line-scans of a hydrated trichome show that there was more oxygen in the base than in the upper part of the trichome (Fig. 4). In contrast, Ca was highly enriched in the upper part of the trichome, with little accumulation in the basal compartment where Zn accumulated. The signal of P also decreased from the top to the base of trichome, indicating that Zn accumulation in the trichome base was not associated with P. Also, S was not present in elevated amounts in the compartment where Zn and Cd accumulated (Fig. 3). Based on the oxygen signal, around half of the trichomes on the leaves of *A. halleri* examined were dehydrated. However, the localisation of Zn and Cd in dead and living trichomes was identical (Fig. 5).

The Zn and Cd accumulation inside the leaf was not homogeneous. The average concentrations in the epidermis were usually two to three times lower than those in the mesophyll cells (Fig. 6). Inside the mesophyll there were few cells which accumulated very high concentrations: up to 70 mM Zn and 10 mM Cd in the 500 µM Zn + 100 µM Cd treatment. In this treatment, mesophyll cells also showed a strong positive linear correlation between the concentrations of Zn and Cd in single cells ($r=0.94$, $P < 0.001$, $n=12$).

The increased Mg concentration in the shoots from the 5 µM Zn + 100 µM Cd treatment, which was phytotoxic, was confirmed by EDXA at the single-cell level: in mesophyll and epidermal cells of this treatment there was a strong ($r=0.79$, $P < 0.0001$, $n=26$) positive correlation between Mg and Cd, with a Mg/Cd ratio of 2.1 (± 0.3 SE). No such correlation was found between these metals in any of the other treatments and other types of cell at the single-cell level. Also, no correlation between Zn and Mg was found.

Increasing external Zn concentrations led to a much greater increase in Zn accumulation in the mesophyll

Table 2. Concentrations of various elements in root tissues of *A. halleri* quantified using EDXA. Standard deviations are in parentheses. For brevity, only two treatments are reported

Treatment	Tissue	Concentration (mM)				
		Cd	Zn	Ca	P	S
500 μM Zn + 100 μM Cd	Rhizodermis (outer wall)	32.9 (46.6)	258.6 (403.3)	16.0 (14.4)	59.7 (58.7)	14.0 (14.0)
	Rhizodermis (vacuole)	1.3 (0.6)	0.4 (0.7)	2.2 (0.9)	5.4 (4.6)	11.2 (6.0)
	Root bark parenchyma	1.1 (0.4)	0.7 (0.9)	1.0 (0.6)	2.9 (2.1)	9.6 (4.1)
	Central cylinder	1.0 (1.3)	0.6 (0.6)	2.2 (2.8)	16.8 (6.4)	5.7 (2.9)
5 μM Zn + 100 μM Cd	Rhizodermis (outer wall)	3.8 (3.0)	0.0 (0.0)	8.9 (5.4)	9.2 (6.5)	12.3 (7.2)
	Rhizodermis (vacuole)	3.6 (2.2)	0.3 (0.5)	5.2 (1.7)	8.6 (8.2)	18.3 (7.7)
	Root bark parenchyma	2.2 (1.1)	0.2 (0.3)	5.2 (4.2)	7.0 (4.7)	8.1 (1.8)
	Central cylinder	1.6 (0.1)	0.0 (0.0)	4.2 (0.5)	11.1 (0.8)	8.2 (1.6)

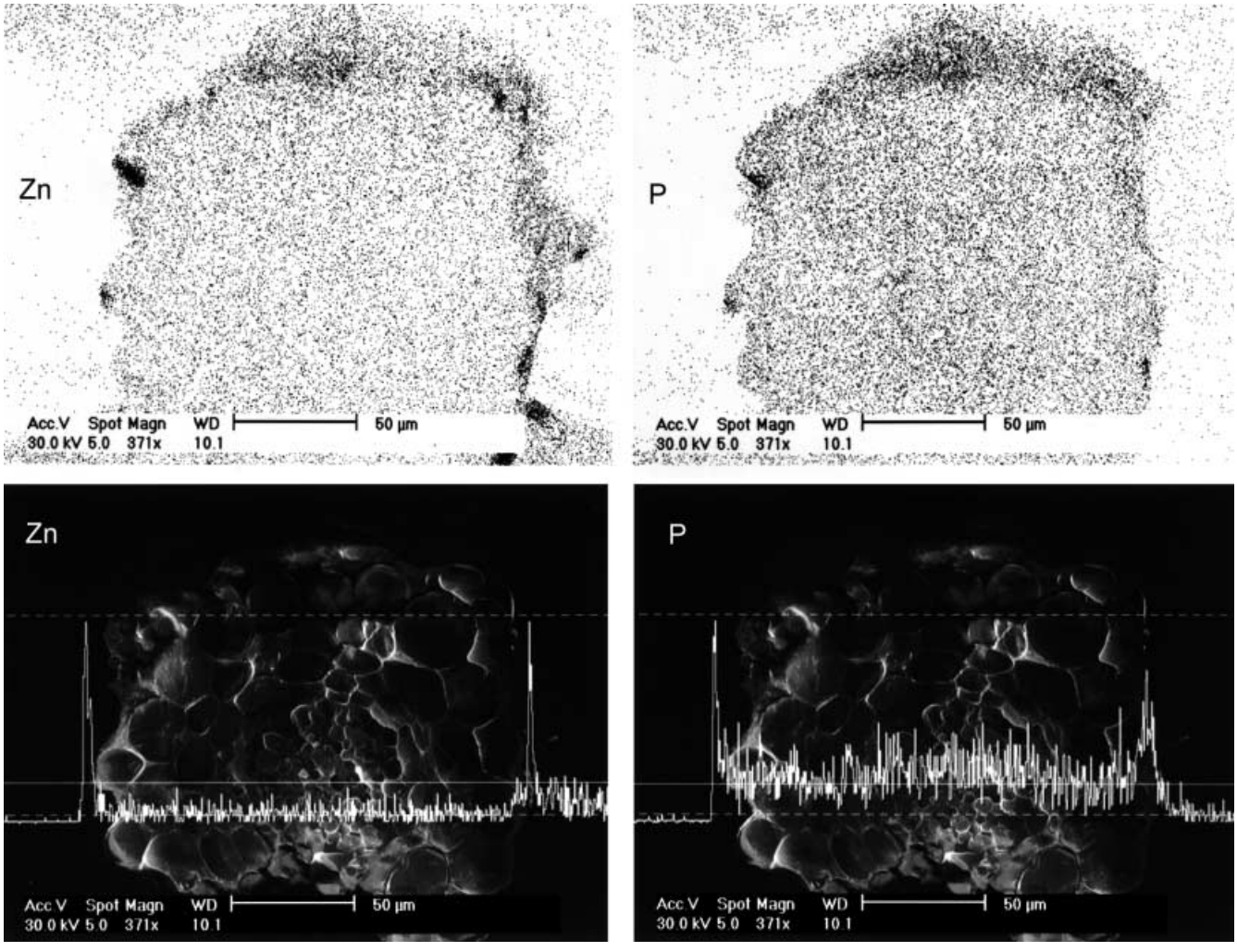

Fig. 2. Precipitations of zinc and phosphorus in the outer cell wall of the epidermis of *A. halleri* roots as shown by a scan of a root cross-section. The analyses were performed in an SEM using an acceleration voltage of 30 kV and a working distance of 10 mm. Dot maps and line scans were obtained by selecting an energy window (0.6 × half-width) inside an X-ray emission line of the element to be measured. *Upper*, dot maps of EDXA counts; *lower*, line scans of EDXA counts; *left*, zinc; *right*, phosphorus

cells than in the trichomes (Figs. 3 and 6). For example, the spongy mesophyll cells in the 500 μM Zn + 100 μM Cd treatment accumulated on average more than 30 mM Zn, representing an increase of more than 30-fold compared to the control. In contrast, concentrations in the trichomes increased by only 3-fold.

In the leaves, the concentration of K was larger in the epidermis than in mesophyll cells, whereas the opposite was observed for Ca (Fig. 6).

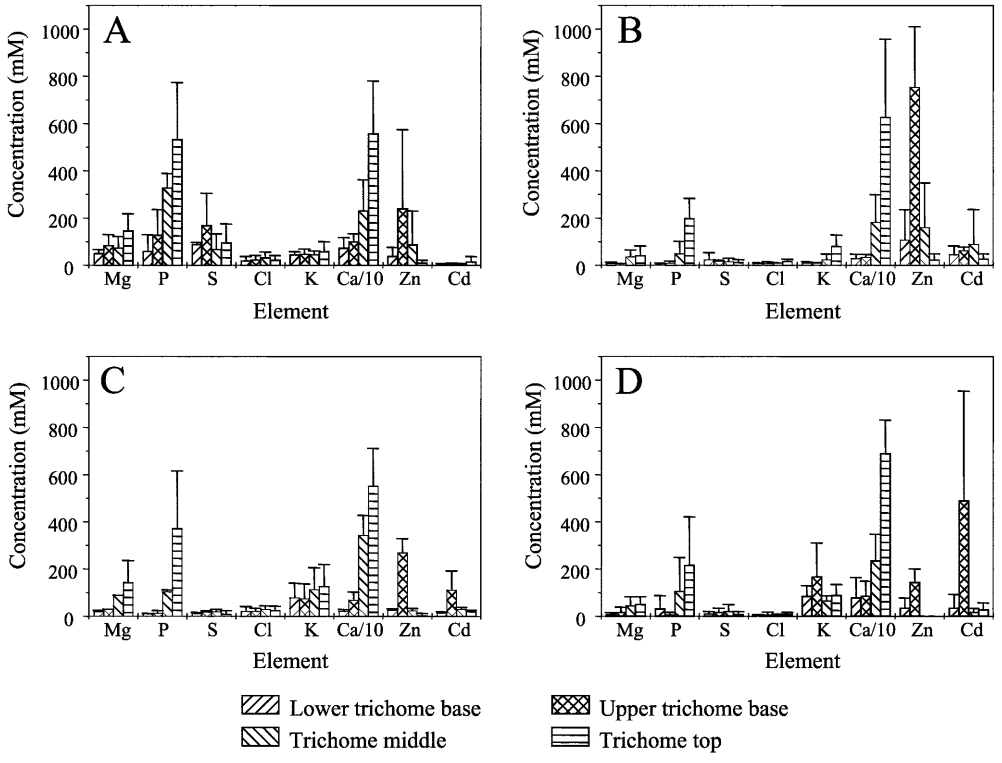

Fig. 3A–D. X-ray microanalysis data from different parts of *A. halleri* leaf *trichomes*. The (apparent) Ca concentrations are divided by 10 to make them fit into the graph and thus enable the comparison of the Ca distribution pattern with that of the other elements. **A** control (5 μM Zn). **B** Grown with 500 μM Zn. **C** Grown with 500 μM Zn + 100 μM Cd. **D** Grown with 5 μM Zn + 100 μM Cd

Flowers. Flowers contained only very small amounts of Zn and Cd, usually at the detection limit of EDXA (i.e. < 5 mM, data not shown). While the concentrations of various elements were not significantly (*t*-test, $P > 0.05$, $n = 53$) changed by the different Zn/Cd treatments, the toxic 5 μM Zn + 100 μM Cd treatment resulted in a reduced size of the flowers as well as a 4- to 5-week earlier blossoming compared to the 500 μM Zn treatment.

Discussion

Zhao et al. (2000) showed that *A. halleri* has accumulation and tolerance capabilities for Zn comparable to the well-known Zn/Cd-hyperaccumulator *T. caerulescens*. The smaller concentration of Zn in shoots, recorded in the present study, in comparison to the results obtained by Zhao et al. (2000) was probably due to the much larger biomass per pot obtained in this experiment (almost 3 times higher). The present study shows that *A. halleri* is also able to accumulate Cd up to almost 6,000 mg kg^{-1} on a dry-weight basis in shoots, although at this level phytotoxicity was observed. No phytotoxicity occurred at a Cd concentration of 2,700 mg kg^{-1} in shoots, suggesting that *A. halleri* can be considered to be a hyperaccumulator of this metal. However, there is no report of Cd hyperaccumulation by *A. halleri* in its natural habitat.

The changes in nutrient balance observed in the 5 μM Zn + 100 μM Cd may be related to the toxic effect of Cd. In fact, the concentrations of Mg and S were significantly enhanced in shoots by this treatment. Furthermore, on the single-cell level a strong positive correlation between Mg and Cd concentrations was found. These observations may be explained by a defence reaction of the plants. The increased Mg concentration may reduce Cd substitution on chlorophyll, which has been shown to be an important damage mechanism in heavy-metal-stressed plants (Küpper et al. 1996). The role of S compounds (i.e. glutathione, phytochelatin) in the detoxification of Cd is well documented (e.g. Steffens 1990; Salt et al. 1995; Kneer and Zenk 1992; Zhu et al. 1999). In contrast, Zn hyperaccumulation in the shoots of *A. halleri* was not associated with S accumulation. The comparison of the two treatments with 100 μM Cd in the nutrient solution revealed that in *A. halleri* increased levels of Zn reduce Cd toxicity by reducing Cd uptake.

Cellular compartmentation of Zn, Cd and other elements in different tissues

The EDXA results provide clear evidence of the precipitation of Zn/Cd phosphates in the apoplast outside the root rhizodermis. This is not surprising because the speciation programme GEOCHEM PC (Parker et al. 1995) predicted formation of Zn/Cd and phosphate precipitates when Zn and Cd in the nutrient solution were at 500 and 100 μM, respectively. Our previous results for plants grown hydroponically also showed a ratio of insoluble Zn to insoluble P in the roots of *A. halleri* that was very close to the stoichiometric ratio of $Zn_3(PO_4)_2$ (Zhao et al. 2000). Further work is needed to elucidate whether apoplastic precipitation of

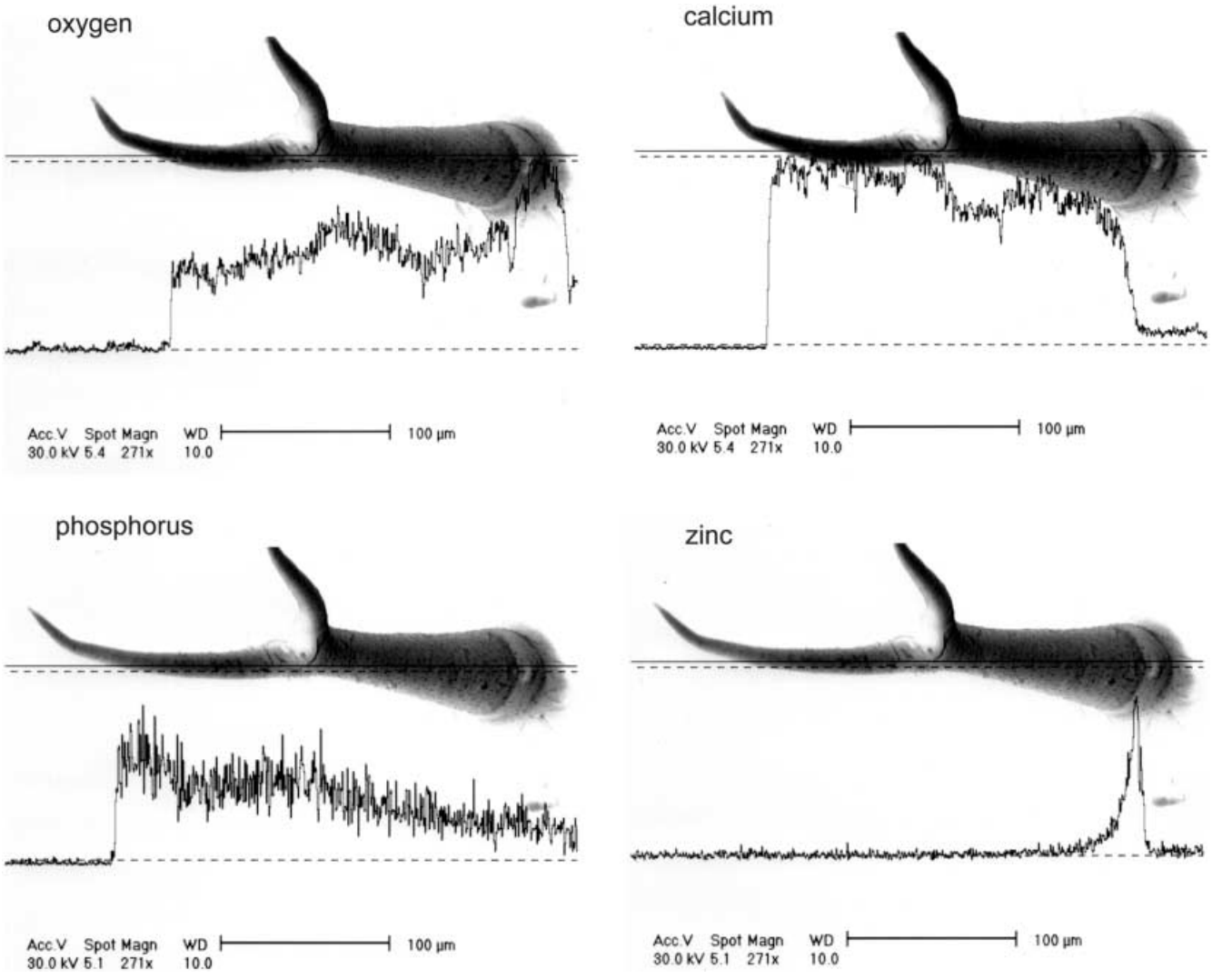

Fig. 4. Distribution of elements in a trichome of *A. halleri* treated with 500 µM Zn. Line scans of EDXA counts of oxygen, calcium, phosphorus and zinc. See Fig. 2 for explanation of SEM parameters

Zn/Cd with phosphate occurs under natural environmental conditions. We think this is unlikely, because the movement of P in the rhizosphere is always limited by diffusion, resulting in depletion rather than accumulation of P at the root surface (Marschner 1995). Depletion of Zn and Cd may also occur in the rhizosphere of hyperaccumulator plants because of their rapid uptake systems (Lasat et al. 2000). Knight et al. (1997) showed that mass flow of Zn and Cd was not enough to account for their uptake by *T. caerulescens* in a range of contaminated soils.

The low concentrations of Zn and Cd in all other parts of the roots are a typical feature of all hyperaccumulator plants as shown by several authors (e.g. Baker et al. 1994; Brown et al. 1995; Shen et al. 1997). Hyperaccumulators usually have a more efficient transport of specific metals from the roots to the shoots in comparison to non-hyperaccumulating plants.

In the leaves of *A. halleri*, trichomes appear to strongly accumulate both Zn and Cd, both being sequestered in a small compartment at the trichome base. This occurred even when the concentrations of Zn and Cd in nutrient solution were relatively low. In a number of other plant species, sequestration of metals in trichomes has been reported, for example lead in *Nicotiana tabacum* (Martell 1974), Cd in *Brassica juncea* (Salt et al. 1995), manganese in *Helianthus annuus* (Blamey et al. 1986), and nickel in the Ni-hyperaccumulator *Alyssum lesbiacum* (Krämer et al. 1997). In particular, Blamey et al. (1986) found that manganese was accumulated in the basal compartment of trichomes in sunflower leaves in a pattern similar to that for Zn/Cd observed in this study. They suggested that trichomes accumulated excess manganese from the surrounding tissues in this species. Part of the manganese can then possibly be secreted as an insoluble oxide. However, in our study, no apparent secretion of Cd or Zn was observed. The chemical forms of Zn and Cd accumulated in the trichome bases of *A. halleri* remain to be determined. Our results indicate that P and S were not

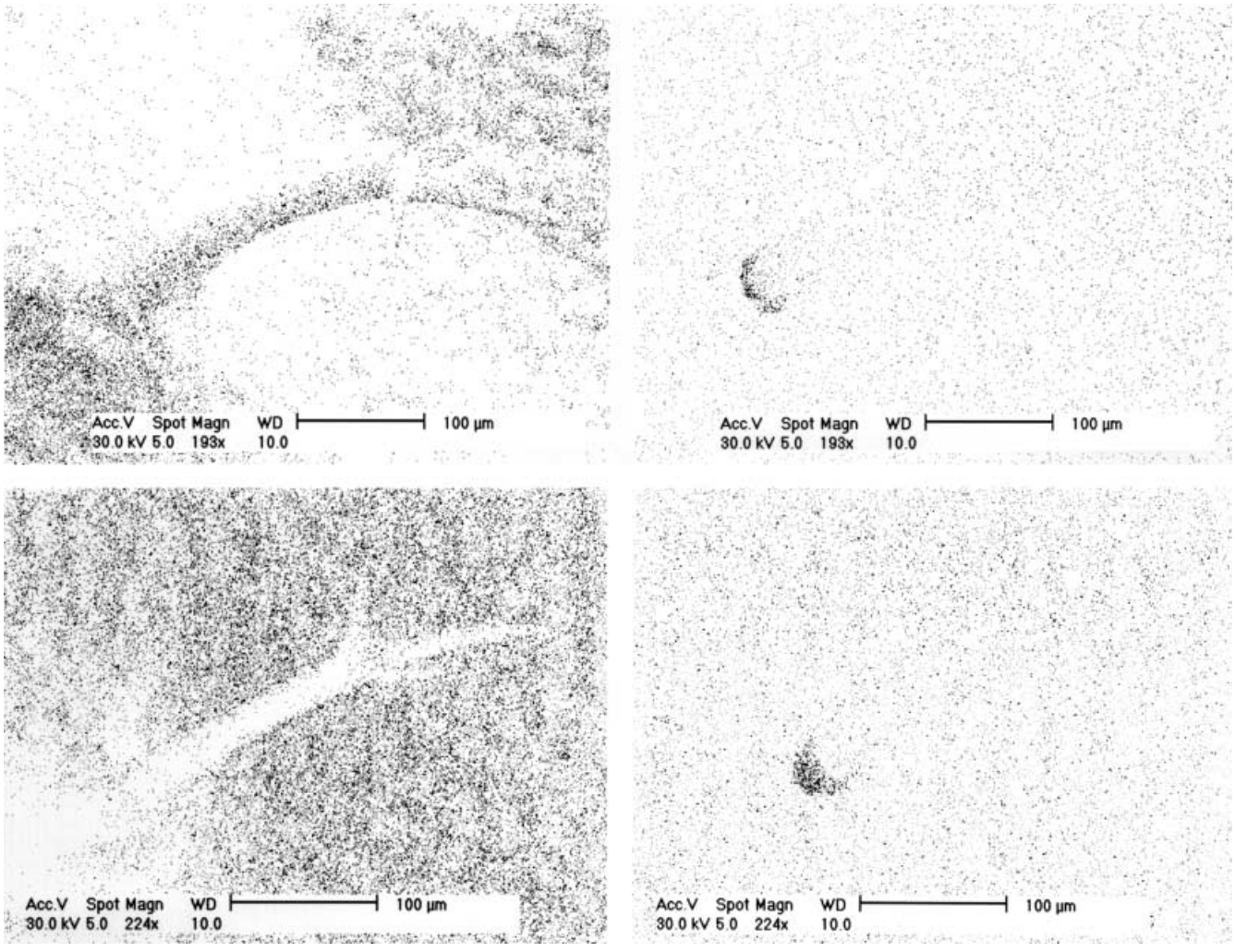

Fig. 5. Distribution of zinc in dead and living trichomes of *A. halleri* treated with 5 µM Zn. Dot maps of EDXA counts. *Upper*, living trichome; *lower*, dead trichome; *left*, distribution of oxygen, showing that the living trichome is hydrated while the dead one is dry; *right*, distribution of zinc. See Fig. 2 for explanation of SEM parameters

involved in the sequestration of the metals. Both metals may be complexed with O-donor ligands such as citrate and present in a soluble form, or more likely as metal oxides in solid forms because of the extraordinary concentrations (>1 M in some cases).

It is clear that trichomes are not the only sink for Zn and Cd in *A. halleri*. Mesophyll cells also accumulated substantial amounts of both metals, most likely in their vacuoles, particularly when the external supply of Zn and Cd was high. In fact, the metal concentrations in mesophyll cells increased much more than the increase in trichomes, suggesting that as hyperaccumulation proceeds to a higher level, mesophyll cells become more important as a sink for Zn and Cd.

In leaves, both Zn and Cd show a very similar pattern of compartmentation (also at the single-cell level), although only Zn is an essential element while Cd, at large internal concentrations, exerts a strong toxic effect on these plants. Because of their chemical similarity, Cd and Zn may be compartmented in a similar way. This seems to involve sequestration of both metals in the vacuoles, keeping the concentrations in the cytoplasm low.

The pattern of cellular distribution of Zn in *A. halleri* leaves differs greatly from that found in *T. caerulescens* (Küpper et al. 1999). In the latter, Zn is accumulated preferentially in the epidermal cells, whereas mesophyll cells have much lower concentrations. The difference between the two species is probably due to the fact that the epidermal cells of *A. halleri*, except trichomes, are very small (8–30 µm in length). In *T. caerulescens*, there is a large variability in epidermal cell size (10–100 µm in length) and Küpper et al. (1999) reported a strong correlation between the size of a cell and its average Zn concentration. This is important in this context because large cells usually have a higher degree of vacuolation than smaller ones in the same tissue. Small sizes of vacuoles in the epidermal cells of *A. halleri* would explain the low accumulation of Zn and Cd in these cells. The pattern of K distribution in the leaf cells of *A. halleri* was also opposite to that observed in *T. caerulescens* (Küpper et al. 1999). Both patterns of

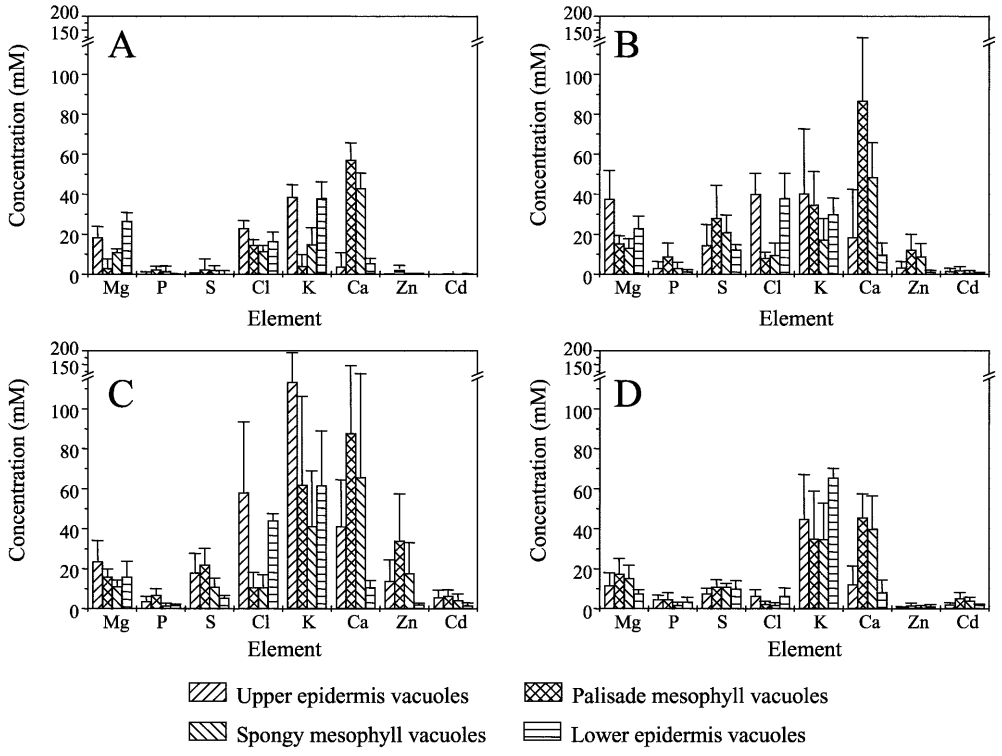

Fig. 6A–D. X-ray microanalysis data from different leaf tissues of *A. halleri*. **A** Control (5 μM Zn). **B** Grown with 500 μM Zn. **C** Grown with 500 μM Zn + 100 μM Cd. **D** Grown with 5 μM Zn + 100 μM Cd

K distribution could be explained by an osmotic adjustment by the plants to balance Zn/Cd in different cell types.

Conclusions

The present work shows the potential for Cd hyperaccumulation in *A. halleri*. This may be of importance for soil remediation technologies based on metal extraction by plants such as phytoremediation (McGrath et al. 2000). Moreover, the results presented here represent the first quantitative study of cellular compartmentation of heavy metals in *A. halleri*. In the root, both Cd and Zn seem to form precipitates with P in the apoplast of the rhizodermis but their concentrations in the rest of the root are generally low. In the leaves the largest concentration of metals was recorded at the base of trichomes. However the mesophyll seems to play an important role in the hyperaccumulation capacity of this species, at least when very large amount of metals are accumulated in the leaves. This result is in contrast to the mechanism of compartmentation reported for the only other known Cd and Zn hyperaccumulator *T. caerulescens*. Further study should specifically address the role of vacuolation in the mesophyll cells in metal detoxification and the relationship, at single-cell level, between metal accumulation and cell damage.

We thank Chris Smith and Phil Jones for technical assistance in using the SEM and EDAX systems, and Sarah Dunham for help with setting up the plant experiments. We gratefully acknowledge financial support from DG XII of the European Commission for the PHYTOREM Project. IACR-Rothamsted receives grant-aided support from the Biotechnology and Biological Sciences Research Council of the United Kingdom.

References

Baker AJM (1981) Accumulators and excluders – strategies in the response of plants to heavy metals. J Plant Nutr 3: 643–654

Baker AJM, McGrath SP, Reeves RD, Smith JAC (2000) Metal hyperaccumulator plants: a review of the ecology and physiology of a biochemical resource for phytoremediation of metal-polluted soils. In: Terry N, Bañuelos G (eds) Phytoremediation of contaminated soil and water. Lewis, Boca Raton, Fla, pp 85–107

Baker AJM, Reeves RD, Hajar ASM (1994) Heavy metal accumulation and tolerance in British populations of the metallophyte *Thlaspi caerulescens* J. & C. Presl (Brassicaceae). New Phytol 127: 61–68

Blamey FPC, Joyce DC, Edwards DG, Asher CJ (1986) Role of trichomes in sunflower tolerance to manganese toxicity. Plant Soil 91: 171–180

Boekestein A, Thiel F, Stols ALH, Bouw E, Stadhouders AM (1984) Surface roughness and the use of a peak to background ration in the X-ray analysis of bio-organic bulk specimens. J Microsc 134: 327–333

Brooks RR (1998) Geobotany and hyperaccumulators. In: Brooks RR (ed) Plants that hyperaccumulate heavy metals. CAB International, Wallingford, UK, pp 55–94

Brooks RR, Lee J, Reeves RD, Jaffre T (1977) Detection of nickeliferous rocks by analysis of herbarium species of indicator plants. J Geochem Explor 7: 49–57

Brown SL, Chaney RL, Angle JS, Baker AJM (1995) Zinc and cadmium uptake by the hyperaccumulator *Thlaspi caerulescens* grown in nutrient solution. Soil Sci Soc Am J 59: 125–133

Kneer R, Zenk MH (1992) Phytochelatins protect plant enzymes from heavy metal poisoning. Phytochemistry 31: 2663–2667

Knight K, Zhao FJ, McGrath SP, Shen ZG (1997) Zinc and cadmium uptake by the hyperaccumulator *Thlaspi caerulescens* in contaminated soils and its effects on the concentration and chemical speciation of metals in soil solution. Plant Soil 197: 71–78

Krämer U, Grime GW, Smith JAC, Hawes CR, Baker AJM (1997) Micro-PIXE as a technique for studying nickel localization in

leaves of the hyperaccumulator plant *Alyssum lesbiacum*. Nucl Instrum Methods Physics Res B 130: 346–350
Küpper H, Küpper F, Spiller M (1996) Environmental relevance of heavy metal substituted chlorophylls using the example of water plants. J Exp Bot 47: 259–266
Küpper H, Zhao FJ, McGrath SP (1999) Cellular compartmentation of zinc in leaves of the hyperaccumulator *Thlaspi caerulescens*. Plant Physiol 119: 305–311
Lasat MM, Baker AJM, Kochian LV (1996) Physiological characterization of root Zn absorption and translocation to shoots in Zn hyperaccumulator and nonaccumulator species of *Thlaspi*. Plant Physiol 112: 1715–1722
Lasat MM, Pence NS, Garvin DF, Ebbs SD, Kochian LV (2000) Molecular physiology of zinc transport in the Zn hyperaccumulator *Thlaspi caerulescens*. J Exp Bot 51: 71–79
Lombi E, Zhao FJ, Dunham SJ, McGrath SP (2000) Cadmium accumulation in populations of *Thlaspi caerulescens* and *Thlaspi goesingense*. New Phytol 145: 11–20
Macnair MR, Bert V, Huitson SB, Saumitou-Laprade P, Petit D (1999) Zinc tolerance and hyperaccumulation are genetically independent characters. Proc R Soc Lond 226: 2175–2179
Marschner H (1995) Mineral nutrition of higher plants. Academic Press, London
Martell EA (1974) Radioactivity of tobacco trichomes and insoluble cigarette smoke particles. Nature 249: 215–217
McGrath SP (1998) Phytoextraction for soil remediation. In: Brooks RR (ed) Plants that hyperaccumulate heavy metals. CAB International, Wallingford, UK, pp 261–287
McGrath SP, Dunham SJ, Correll RL (2000) Potential for phytoextraction of zinc and cadmium from soils using hyperaccumulator plants. In: Terry N, Bañuelos G (eds) Phytoremediation of contaminated soil and water. Lewis, Boca Raton, Fla., pp 109–128
Parker DR, Norvell WA, Chaney RL (1995) GEOCHEM-PC – A chemical speciation program for IBM and compatible personal computers. In: Loeppert RH, Schwab AP, Goldberg S (eds) Chemical equilibrium and reaction models. Soil Science Society of America, American Society of Agronomy, Madison, Wis., pp 253–269
Salt DE, Prince RC, Pickering IJ, Raskin I (1995) Mechanisms of cadmium mobility and accumulation in Indian mustard. Plant Physiol 109: 427–433
Salt DE, Smith RD, Raskin I (1998) Phytoremediation. Annu Rev Plant Physiol Plant Mol Biol 49: 643–668
Salt DE, Prince RC, Baker AJM, Raskin I, Pickering IJ (1999) Zinc ligands in the metal hyperaccumulator *Thlaspi caerulescens* as determined using x-ray absorption spectroscopy. Environ Sci Technol 33: 712–717
Salt DE, Kato N, Krämer U, Smith RD, Raskin I (2000) The role of root exudates in nickel hyperaccumulation and tolerance in accumulator and nonaccumulator species of *Thlaspi*. In: Terry N, Banuelos G (eds) Phytoremediation of contaminated soil and water. Lewis, Boca Raton, Fla., pp 189–200
Shen ZG, Zhao FJ, McGrath SP (1997) Uptake and transport of zinc in the hyperaccumulator *Thlaspi caerulescens* and the non-hyperaccumulator *Thlaspi ochroleucum*. Plant Cell Environ 20: 898–906
Steffens JC (1990) The heavy metal-binding peptides of plants. Annu Rev Plant Physiol Plant Mol Biol 41: 553–575
Tomos AD, Hinde P, Richardson P, Pritchard J, Fricke W (1994) Microsampling and measurements of solutes in single cells. In: Harris N, Oparka KJ (eds) Plant cell biology – a practical approach. IRC Press, Oxford, pp 297–314
Van Steveninck RFM, Van Steveninck ME (1991) Microanalysis. In: Hall JL, Hawes C (eds) Electron microscopy of plant cells. Academic Press, London, pp 415–455
Zhao FJ, Lombi E, Breedon T, McGrath SP (2000) Zinc hyperaccumulation and cellular distribution in *Arabidopsis halleri*. Plant Cell Environ 23: 507–514
Zhu YL, Pilon-Smith EAH, Tarum AS, Weber SU, Jouanin L, Terry N (1999) Cadmium tolerance and accumulation in Indian mustard is enhanced by overexpressing γ-glutamylcysteine synthetase. Plant Physiol 121: 1169–1177